Influence du mode d'accès proprioceptif sur un principe de contrôle

Coping with decline of visual and proprioceptive sensory processing in interception

Abstract

We investigated the contribution of proprioceptive information to the human ability to perform interceptive action on the basis of the Constant Bearing Angle strategy (CBA) depending on the availability of visual allocentred and/or egocentred perceptual-motor variables in the visual environment. In an experiment run in virtual reality, a deafferented patient (Patient GL) and age-matched healthy control participants (Middle-Aged) were required to control their forward velocity with a joystick in order to intercept ball moving toward them obliquely. Participants were exposed to four visual environments that provided either allocentred and egocentred perceptual-motor variables (*Full* Environment), only allocentred (*Ground* Environment), only egocentred (*Landmark* Environment) or none of them (*Empty* environment). The results indicated that the Patient GL experienced more difficulties in performing the task, in comparison with Middle-Aged participants. Moreover, Patient GL produced much more jerky velocity adaptations in comparison with Middle-Aged participants. The “Bounded-CBA” model, taking into account putative increased perceptual thresholds due to ageing and pathology provided a better account of the regulations exhibited by the Middle-Aged and the Patient GL than the original CBA model in the different environment conditions. The implications of this study to a better understanding of the mechanisms underlying the detection of the rate of change in bearing angle are discussed.

INTRODUCTION

How can a given perception-action mechanism be used by living agents through life despite age and pathology-related decline in sensory processing? We tried to answer to this question by focusing on the respective contribution of proprioception and vision to perform interceptive actions on the basis of the ‘B*ounded - Constant Bearing Angle (Bounded-CBA)*’ strategy formulated by Francois, Morice, Blouin et Montagne (in press). We investigated the performance and kinematics of the Deafferented Patient GL and his/her Middle-Aged healthy counterparts’ depending on the availability of visual allocentred and/or visual egocentred perceptual-motor variables.

In the perception-action framework (Gibson, 1998), the success of goal directed actions is guarantied when living agents (i.e., humans, animals) take advantage of the perceptual information available from the visual and proprioceptive sensory signals produced by their displacements, so as to produce on-line locomotor adjustments. Such on-line coupling between movement and information has been formalized through task-specific laws of control (Warren, 1988, 2006). These laws of control rely on the assumption that the perceptual information picked up by agents specify the current state of the relationship linking an agent to his/her environment and thus informs he/she about the direction of regulation to produce so as succeeding in the considered task. In other words, agents would use an information that allow the perception of invariant properties of the agent-environment relationship in order to produce functional locomotor adjustments’, which in turn would modify the information, and so on and so forth. Task-specific laws of control have been evidenced to account for the regulation behavior of participants in heading tasks (Warren, Kay, Zosh, Duchon, & Sahuc, 2001; Wilkie & Wann, 2003), locomotor pointing tasks (Warren, Young, & Lee, 1986) or interceptive tasks (Bootsma, Fayt, Zaal, & Laurent, 1997; Chardenon, Montagne, Laurent, & Bootsma, 2004).

Interceptive tasks have deserved a special interest, not only because many daily activities rely on the ability to intercept and/or to avoid moving objects (in sport, in driving, or while walking in a crowded street), but also because they can provide insights about the central control of actions characterized by strong spatio-temporal constraints. It has been suggested that observers intercepting moving targets rely on a law of control called ‘Constant Bearing Angle (CBA)’ strategy. The CBA strategy allows succeeding in interceptive action by performing on-line regulation of kinematics in order to cancel the value of the rate of change of the bearing angle, that is the angle subtended by the current position of the target to be intercepted and the direction of the observer' motion (Chapman, 1968; Chardenon, Montagne, Buekers, & Laurent, 2002 ; Lenoir, Musch, Thiery, & Savelsbergh, 2002, see Figure 55).

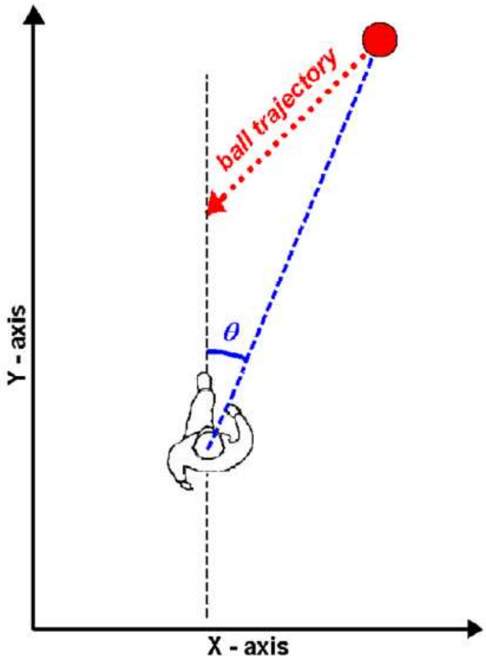

Figure 55: Top view of the agent-environment relationship during interceptive actions. Participants produce forward displacements on a rectilinear path and aim to intercept balls that cross their displacement axis with an angle of 45°. Optical angle of interest for the Constant Bearing Angle strategy is the bearing angle θ .

The principle of the CBA strategy holds that the rate of change of the bearing angle ($\dot{\theta}$) directly specify to the observer if its current velocity will allow him/her to intercept moving target or if velocity regulations (i.e., acceleration or deceleration) are necessary. A positive $\dot{\theta}$ (i.e., an increase of the bearing angle as a function of time) informs the observer that the target will cross his/her axis of displacement behind him/her and tells him/her to decelerate accordingly. Conversely, a negative $\dot{\theta}$ (i.e., a decrease of the bearing angle) informs the observer that the target will pass his/her axis of displacement in front of him/her and prompts him/her to accelerate accordingly. Finally when $\dot{\theta}$ is null (i.e., the bearing angle is kept constant as a function of time), no participant's acceleration or deceleration is required to intercept the target. The use of the CBA strategy has been evidenced by revealing specific signatures of human kinematics when task constraints such as ball speed Chardenon, Montagne, Laurent, & Bootsma, 2005; Lenoir et al., 2002), angle of approach (Chardenon et al., 2005) or ball trajectory curvature (Bastin et al., 2006b) were manipulated. In these studies, the CBA strategy was modeled by relating the participant's acceleration to the rate of change of the bearing angle ($\dot{\theta}$, Equation 1), with a damping term allowing the system to match the required value smoothly and to avoid oscillations around the stable state (Bastin et al., 2006b; Fajen & Warren, 2003; Wann & Wilkie, 2004). Then, modeling kinematics according to the CBA law of control could explain as much as 80 % of the total kinematics variance.

$$\ddot{Y} = k_1 \times \frac{1}{1 + 200 \times e^{(-10 \times t)}} \times \dot{\theta} + k_2 \times \dot{Y} \qquad \text{Equation 1}$$

In this equation, $\dot{Y}$ and $\ddot{Y}$ are the participant's speed and acceleration along the Y-axis (*cf.*, Figure 55), respectively, $\dot{\theta}$ is the rate of change of the bearing angle, k_1 is a parameter that modulates the strength of the coupling between the acceleration and the rate of change of the bearing angle, and k_2 is a parameter that modulates the strength of the damping term. The function $\frac{1}{1 + 200 \times e^{(-10 \times t)}}$ is an activation function. Interestingly, the CBA strategy seen to be exploited by a large span of living agent ranging from children (from 10 to 12 years old) intercepting moving balls (Chohan et al., 2008) to animal species (fishes, dragonflies) intercepting prey (Lanchester & Mark, 1975; Olberg et al., 2000).

From a perceptual view point, two different frames of reference have been suggested in order to sort the different sensory modalities and perceptual variables that could be used by agent to detect $\dot{\theta}$: (a) an allocentric frame of reference is used when target angular position is determined in relation to invariant properties of the environment surrounding the target and/or (b) an egocentric frame of reference is used when the angular position of the ball is determined in relation to the position of the body. On the one hand, visual signals provide at least two perceptual variables allowing to perform an allocentric detection of $\dot{\theta}$. The first visual variable identified as a power source of information for detecting $\dot{\theta}$ is provided by the global optic flow field produced by the moving observer. The global optic flow field contains a visual property, the Focus of Expansion (FoE), that invariantly specifies to the observer his/her direction of motion. Thus, an easy way to perform interceptive action consists in cancelling the current angular position of the target regarding to the FoE. Other visual variables can be used to encode $\dot{\theta}$ if the visual environment contains a structured background. For instance, moving so as to keep the same distant object occluded by the target would also lead to the interception of the target (in this case, θ and $\dot{\theta}$ are kept around null values). On the other hand, both proprioceptive and visual signals can be used to perform an egocentric detection of $\dot{\theta}$. Indeed, proprioception coming from the vestibular apparatus, the extra-ocular muscles and/or from neck muscles (Blouin et al., 2007; Jeannerod, 1991; Paillard, 1987) provides body-related-signals that could be used as a reference frame for detecting the angular position of the ball. Thus, an easy way to perform interceptive action consists in cancelling the current angular position of the target regarding to the body midline axis. Vision can also provide a perceptual variable when body-fixed visual references, or landmarks are present in the environment (e.g., a dashboard or a car's bonnet when driving, a handlebar when cycling) (Wilkie & Wann, 2002).

From a sensory processing point of view, the weighting of the visual and proprioceptive signals for encoding $\dot{\theta}$ appears highly context-dependent. Taken together, the following studies have shown that not only the different sensory modalities (i.e., vision, proprioception) but also different perceptual variables provided by a sole sensory signal (i.e., FoE, Landmark) contribute jointly to the detection of the rate of change in bearing angle. The visual allocentric encoding of $\dot{\theta}$ would have the greatest weight when the visual environment is well structured Bastin & Montagne, 2005; see Warren et al., 2001 for a similar result wittth heading tasks). In visually impoverished environments, the proprioceptive egocentric encoding of $\dot{\theta}$ would gain in importance (Bastin et al., 2006b). Moreover, the accuracy with which participants use a visual egocentric encoding of $\dot{\theta}$ can be improved when body-fixed visual references are present in the environment (Wilkie & Wann, 2002).

From a methodological view point, studies that have been designed to determine how sensory modalities (i.e. vision, proprioception) and perceptual-motor variables (i.e., FoE, Landmark) are integrated for detecting $\dot{\theta}$ are all based on the same experimental paradigm consisting in decorrelating a given source of information from the property specified (i.e. rendering irrelevant a given source of information informing the participant about its axis of displacement/body axis) and recording the behavioral consequences of this experimental manipulation. Decorrelation has been tested with visual signals allowing the allocentric detection of $\dot{\theta}$. In this case, the FoE has been decorrelated from the actual direction of displacement by laterally displacing the ground plane during self displacement in virtual reality (Chardenon et al., 2004). Decorrelation has been tested with visual signals allowing the egocentric detection of $\dot{\theta}$. For instance, decorrelating a visual variable form its specification of the midline body axis has been achieved by laterally displacing visual landmarks materializing the midline body axis (Bastin & Montagne, 2005). Decorrelation has finally been tested with proprioceptive egocentric encoding of $\dot{\theta}$. For instance, decorrelating a proprioceptive variable from the actual midline body axis has been achieved by vibrating the neck muscles (Bastin et al., 2006a).

Studying specific populations of humans (e.g., Young vs. Middle-Aged) might provide interesting insight in the understanding of flexibility of sensory processing. Recently Francois, Morice, Blouin et Montagne (in press) have shown that Middle-aged participants continue to exploit the CBA strategy despite age-related decline in their sensory accuracy. More precisely, the authors showed that participant's kinematics could be modeled by the CBA strategy provided that some perceptual thresholds accounting for aged-related decline in visual and proprioceptive encoding of $\dot{\theta}$ are integrated in the CBA model architecture. Studies of deafferented human patients might provide complementary piece of answer to the understanding of sensory processing flexibility through life. If proprioception from the neck muscles for instance is only required for detecting $\dot{\theta}$, one could ask whether these patients are able to intercept moving balls in impoverished visual environments and to achieve interception scores similar to those of age-matched healthy control. If the performance differs between the healthy subjects and these patients, this would indicate the importance of non-visual information for detecting the bearing angle. On the other hand, similar ability to intercept a moving object between the healthy and the Patients would attest to the power of visual information in the control of self-displacement.

In the present study, we run an experiment in virtual reality in which participants were required to intercept ball moving toward them obliquely. The first aim of the study was to test the importance of the proprioceptive egocentric detection of $\dot{\theta}$ depending on the kind of visual information available (i.e., both egocentric and allocentric, only allocentric, only egocentric, none of them), we compared the performance and kinematics of a deafferented Patient GL suffering from a severely impaired egocentric frame of reference to his/her *Middle-Aged* counterparts in a virtual interceptive task. The second (related) aim of the study was to test to what extent the 'Bounded Constant Bearing Angle' strategy formulated by Francois et al. (in press) could account for the locomotor adjustments produced by the deafferented Patient GL.

METHOD

Participants

Seven females, self-declared right-handed and having normal or corrected-to-normal vision participated to the experiment. They were divided into two experimental groups: a deafferented Patient GL with large-fibre sensory neuropathy (N= 1, 59 years old, called 'Patient GL') and age-matched healthy control (N = 6, 57.8 ± 2 years old, called 'Middle-Aged'). At the age of 31, after a severe sensory polyneuropathy, the *Patient GL* incurred the loss of the large myelinated fibers. Since then, she has an acute loss of all somatosensory modalities (*e.g.*, kinesthesia, tendon reflexes, touch, vibration and pressure) from her nose to her feet, thus including the cervical region. Her vestibular system remained normal as attested by vestibulo-ocular reflex measurement (Blouin, Vercher, Gauthier, Paillard, Bard, & Lamarre, 1995) and her efferent motor pathways are also normal. Although confined to a wheelchair, the *Patient GL* can perform most daily activities with concentration and visual feedback. Due to her impaired egocentric frame of reference, however, her motor performance decreases in visually unstructured visual environments (Blouin, Bard, Teasdale, Paillard, Fleury, & Forget, 1993). A detailed clinical history of the *Patient GL* have been published elsewhere (Cooke, Brown, Forget, & Lamarre, 1985; Forget & Lamarre, 1995). All participants gave their informed consent before participating in the experiment. A local ethics committee approved the experimental protocol.

Apparatus

The virtual reality set-up is depicted on Figure 56. Participants seated 0.70 m in front of a 2.3-m high × 3-m wide projection screen (117° × 130° field of view) and held an analog 2-directions joystick (Happ Controls, Inc. in Elk Grove Village, IL, United States) in their right hand[19] with their arm resting on a table. Participants could increase (decrease) their forward acceleration by pushing (pulling) the joystick from the neutral initial position up to an acceleration (deceleration) of 0.75 m/s^2 (-0.75 m/s^2). Resulting speed was bounded from -0.8 m/s to 3.2 m/s (i.e., ≈ human span of walking speed). When the joystick remained in neutral

[19] Despite allowing 2D movements, sole the frontward/backward movements of the joystick gave rise to visual consequences in our VR apparatus.

position, no acceleration or deceleration occurred and the current velocity was kept constant. Participants wore goggles to prevent them from seeing both the joystick and their own hands. The acceleration provided by the joystick was sampled at 200 Hz and sent in real time to an acquisition system (ADwin-Pro, Keithley Instruments, Inc., Cleveland, OH, United States) that allowed a first host computer to integrate twice time the acceleration signal provided by the joystick in order to compute on-line the position of the participant in the virtual world. This position data was sent to a second host computer which generated the visual scene and rear-projected it onto the projection screen by the video projector (IQ R500, Barco, Inc., Duluth, GA, United States).

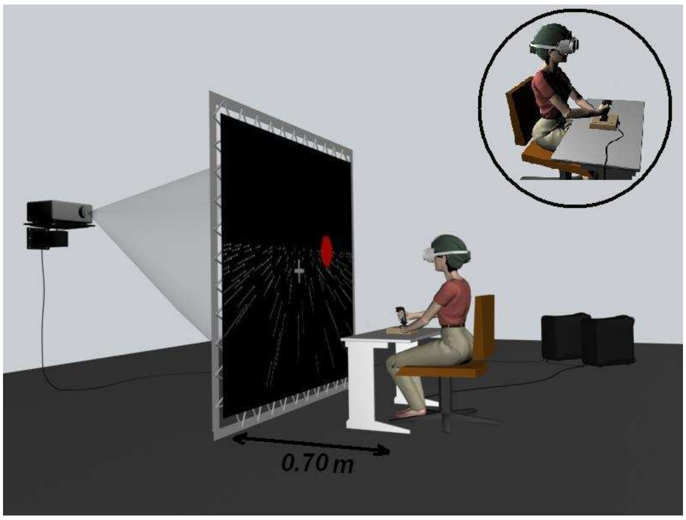

Figure 56 : Virtual reality set-up for ball interception used in the experiment. Participants seated in front of a large projection screen and controlled their displacement acceleration via a joystick. Resulting acceleration was integrated two times and coupled to the rear-projected visual scene. All participants wore goggles that prevented them from seeing their hand and the joystick position. The Patient GL' hand was fixed to the joystick by mean of a Velcro so that she always grasped the joystick despite never seeing it.

Experimental procedure

The experiment was divided into three sessions. The first session allowed the participants to calibrate themselves with the joystick action and with its visual consequences. In this 3-minutes session, participants were immersed in a virtual corridor and were instructed to regulate their velocity so as to keep a constant distance between them and a large virtual textured ball (2 m diameter) rolling on the floor along a straight line at varying velocities (from 0.52 to 3.82 m/s). All participants showed no difficulties in performing this task.

The second session was designed to familiarize the participants with the experimental task. Participants were asked to produce forward displacements in the virtual environment and were instructed to intercept the balls (red untextured spheres, 0.22 m diameter), which moved toward them obliquely at eye level. They were simply instructed to regulate their velocity in order to intercept the balls with their head when the balls crossed their displacement axis. At the end of each trial, the participants were informed of the distance separating their head from the ball when it crossed their axis of displacement. Positive and negative signs were given when the ball crossed the axis in front or behind the participants, respectively. This session lasted 10 minutes.

The third session was the experimental session and task requirements remained unchanged compared with the task familiarization session. However, no knowledge of results regarding the participants' performance was provided.

Independent variables

In both the familiarization and experiment tasks, we manipulated the offset of the ball (three modalities: -2.5 m, +0.2 m and +2.5 m). The three different offset modalities corresponded to three ball arrival position along the subject's displacement axis (i.e., 5.5, 8.2 and 10.5 m in front of the participant departure, Figure 57A), diminishing thus the possibility of predicting the interception point from the start of the trial, and favoring thus the online control of the displacement velocity. As consequences of the three offsets modalities, keeping the initial displacement velocity (set at 1 m/s) unchanged, would result in the ball passing respectively 0.2 m and 2.5 m in front of the head of the participants for the +0.2 m and +2.5 m offset modalities, and 2.5 m behind their head in the -2.5 m offset modalities.

We also manipulated the visual content of the virtual Environment (four modalities: *Full*, *Ground*, *Landmark* and *Empty*) in both the familiarization and experiment tasks. In the *Empty* condition, only the ball was visible (Figure 57B). In the *Landmark* condition, a grey cross (0.2 m × 0.2 m) depicting the midline body axis (which coincided with the axis of displacement) appeared on the screen at about shoulder level. In the *Ground* condition, the ground plane was textured (extensionless, randomly distributed dots, 0.65 dots/m^2). Finally, in the *Full* condition, the cross and the textured ground plane were displayed. The 12 experimental conditions (3 Offsets × 4 Environments) were repeated ten times each, giving rise to a total of 120 trials. Finally, Experiment 1 was composed of 120 trials, randomly presented for each participant: (12 trials × 3 Offsets[-2.5, +0.2, +2.5 m] × 4 Environments[*Full*, *Ground*, *Landmark*, *Empty*]) and spent 30 minutes long.

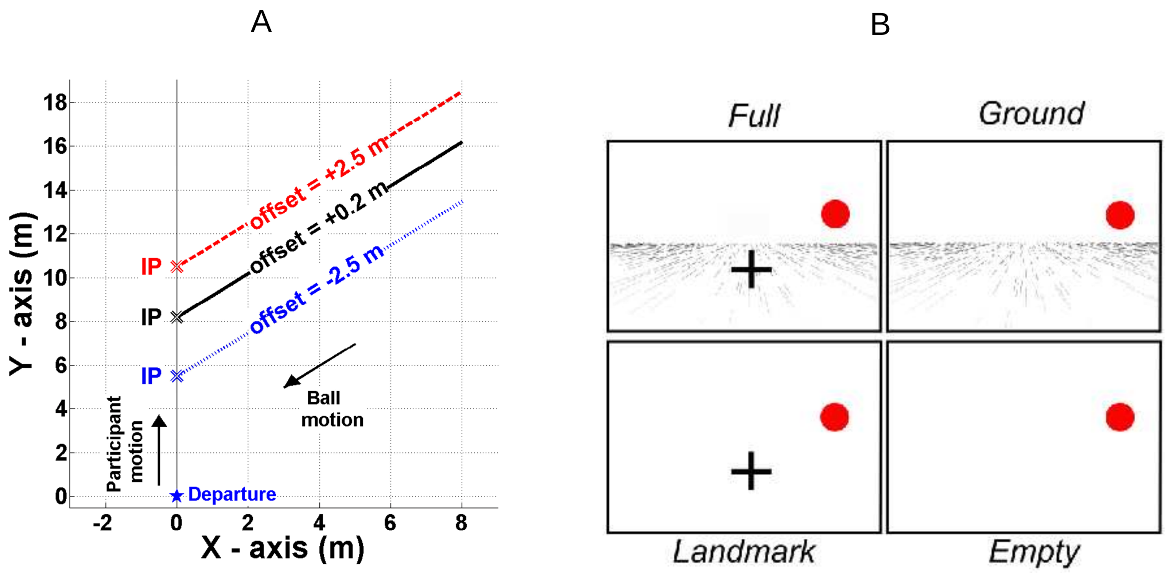

Figure 57 : (A) Top view of the ball trajectory and ball arrival position (i.e. interception points *IP*), participant departure and direction of displacement as a function of the three offset conditions (in dotted, plain and dashed lines for the *-2.5*, *+0.2* and *+2.5 m* offset conditions, respectively). (B) Visual scene appearance in the four environment conditions (*Full*, *Ground*, *Empty* and *Landmark*). Screenshots are depicted with inversed colors.

Data analysis and dependent variables

The data were analyzed with regard to performance outcome, movement kinematics and perceptual-motor strategies involved.

Performance

Performance was computed in two different ways. The final Y-positions of participants along the Y-axis were cumulated and the percentages of trials displaying undershoots or overshoots of the interception point (IP) were computed. The absolute error (AE) was computed as the Euclidian distance between the centre of the head and the centre of the ball. Two different methods were used to compute participant to ball distances in AE: (1) at the moment at which the ball crossed the axis of displacement (i.e., 8 s after the ball appearance) or (2) at any moment during the trial.

Kinematics

The time series of individual velocity ($\dot{Y}$) profiles were averaged over intervals of 500 ms giving rise to 16 time intervals (see Bastin et al., 2006a, 2008; ; François et al., in press; Morice, Francois, Jacobs, & Montagne, 2010; Warren et al., 2001, for a similar methodology). Acceleration ($\ddot{Y}$) profiles were analyzed so as to identify the number of zero-crossings ($ZC_{\ddot{Y}}$). The number of zero crossings reflects the number of successive acceleration/deceleration cycles during the displacement and was used to determine the number for velocity regulation during a trial time course. For each acceleration profile (individual mean acceleration profiles for *Middle-Aged* Participants and trial acceleration profiles for the *Patient GL*), we picked out the number of zero crossings (from 1 to 5) during the trial time course and expressed it as a percentage of the total number of $ZC_{\ddot{Y}}$, so as to compare the two groups of participants.

Perceptual-motor strategy

Subsequent analyses compared the kinematics predicted by the CBA and by the 'Bounded-CBA' models (Francois et al., in press) with the observed kinematics computed by averaging individual displacement velocity profiles recorded for each group. Predicted kinematics were obtained as follow. The best-fitting set of parameters k_1 and k_2 (Equation 1) were first determined separately for each Offset, Environment, Group and model. Forty hundred combinations of parameter values were used (k_1 was varied from -0.95 to 0 in increments of 0.05 and k_2 from 0.0 to 0.95 in increments of 0.05). The initial mean position and speed of the participant and target were used as input variables. Numerical simulations were done on the complete trial duration (*i.e.*, 8 s). The goodness of the observed data's fits provided by predicted kinematics were investigated through both the percentages of variance accounted for (R^2) and the Sum of Squares Error (SSE) between the predicted and observed curves. Predictions were thus obtained for each group, experimental condition and model. Secondly, the best set of k_1 and k_2 parameters, common for all offset conditions, but customized to each group, environment and model was determined separately by comparing the SSE between best predicted and observed kinematics.

Statistics

For each dependant variable, either individual mean values computed from *Middle-Aged* participants or trial values computed from the *Patient GL* were submitted to analyses of variance (ANOVA)[20].

Discrete variables (Absolute Error (AE) and Zero Crossings ($ZC_{\ddot{Y}}$)) The effect of Environment conditions on AE and $ZC_{\ddot{Y}}$ on *Middle-Aged* participants and the *Patient GL* were tested with separate one-ways ANOVAs (4 Environments) with repeated measures on the Environment conditions [Full, Ground, Landmark and Empty].

Kinematics

Separate three-ways ANOVAs with repeated measures on Environments [Full, Ground, Landmark and Empty], Offsets[21] [-2.5, 0.2 and +2.5] and Time Intervals [16 intervals] conditions were performed on displacement velocity profiles for each group (*Middle-Aged*, *Patient GL*).

Comparing the Patient GL with Middle-Aged participants:

To compare the *Patient GL*'s data with those of *Middle-Aged* participants, the individual mean values obtained by the *Patient GL* in each dependent variable was converted to z-scores on the basis of mean and standard deviation of the *Middle-Aged* individual values. We considered that the *Patient GL*'s results differed significantly from those of *Middle-Aged* participants when her z-scores fell outside the 95% confidence intervals of the *Middle-Aged* participants for each dependent variable (AE, $ZC_{\ddot{Y}}$ and velocity).

Post hoc comparisons were conducted using Newman-Keuls tests. The *p* value for statistical differences was set at 0.05.

---

[20] 10% of trials were excluded for each group. (AE>1.1 m for *Middle-Aged* participants and AE>1.8 m for the *Patient GL*). Remaining trials were all analysed.

[21] As mentioned previously, the manipulation of the offset condition was introduced in order to favor the online control of the displacement velocity. As a consequence, no effect of the offset factor on performance was expected and this factor was not included from statistical analyses. Conversely, an effect on kinematics was expected and the factor offset was introduced in the analyses.

Predictions

The considered CBA strategy is based on the participant's ability to detect and cancel the rate of change of the bearing angle ($\dot{\theta}$). Perceiving $\dot{\theta}$ imply to rely on the combination of visual signals (to see the ball) and different sensory modalities (i.e., vision, proprioception) and different perceptual variables (i.e., FoE, Landmark) depending on the frame of reference used (i.e., allocentric, egocentric). Specific predictions about the way of perceiving $\dot{\theta}$ can thus be made depending on Environment manipulation and groups of participant~~s~~.

Concerning the effect of Environment manipulations, in the *Empty* modality $\dot{\theta}$ could only be determined by using an egocentric frame of reference combining the visual position of the ball to extra-retinal signals (e.g., proprioception and oculomotor). This remains available in all Environment conditions. In the *Landmark* modality, $\dot{\theta}$ could only be determined by using an egocentric frame of reference combining the visual position of the ball to visual information of the body axis (e.g., the landmark) or to extra-retinal signals (e.g., proprioception and oculomotor). In the *Ground* modality, $\dot{\theta}$ could be determined by using an egocentric frame of reference combining the visual position of the ball to extra-retinal signals (e.g., proprioception and oculomotor) or by using an allocentric frame of reference combining the visual position of the ball to the visual position of the FoE. In the *Full* modality, all previously cited sensory signal and perceptual variables can be used to rely on the egocentric and allocentric frames of reference.

Concerning the effect of Group manipulation, the literature revealed that the different types of perceptual signals are redundant since they allow interceptive tasks to be performed whatever the perceptual content of the environment for healthy participants. The age-related decrease in performance of *Middle-aged* participants was described by Francois et al. (in press). We thus focus on the effect of deafferentation. The lost of somatosensory modalities should prevent the *Patient GL* to use proprioception to detect her direction of displacement. This allows us to predict an interaction between the Environment and the Groups. Indeed, in the *Empty* condition the *Patient GL* should not use proprioceptive information to rely on an egocentric frame of reference and would experience difficulties in intercepting the ball. Conversely, when visual signals are available (i.e., in the *Landmark, Ground* and *Full* conditions), the *Patient GL* should be able to use egocentric and allocentric frame of reference to reach a similar level as *Middle-Aged* participants. Finally given the impossibility for the *Patient GL* to track the ball angular position without using at least one of visual information concerning its direction of displacement (i.e., FoE or Landmark), it's also reasonable to anticipate that the behavior produced by the Patient GL, should be jerkier than the behavior produced by Middle-Aged participants.

RESULTS

Performance

Absolute Errors

The panel A of the Figure 58 depicts the frequency distributions of participant's final Y-positions (*i.e.*, participant's positions along the Y-axis at time t=8 s, when the ball crossed the participant's displacement axis) cumulated across trials and Environment conditions for the three offset conditions as compared to the position of the Interception Point (IP equal to 5.5, 8.2 and 10.5 m for the -2.5, +0.2 and +2.5 m Offset conditions). For all Offset conditions, the frequency distributions of *Middle-Aged* participant's final Y-positions presented Gaussian shapes and were spread up forward and backward the IP, whereas the *Patient GL* distributions of final Y-positions appeared flat and randomly binned forward and backward the IP. On average, distributions of final Y-positions show that *Middle-Aged* participants and the *Patient GL* similarly overshoted the IP (56.47 vs. 56.92 % of trial) in the three offset conditions (final Y-positions equal to 5.57, 8.24 and 10.51 m vs. 5.61, 8.39 and 10.57 m for *Middle-Aged* participants and the *Patient GL*, respectively)

The panel B of Figure 58 displays the absolute errors (AE) computed in two ways for the two groups (*Middle-Aged*, *Patient GL*) in the different Environment conditions (*Full*, G*round*, *Landmark, Empty*). We first considered absolute errors as the Euclidian distance between the agent and the ball at the moment at which the ball crossed the participant's displacement axis (dotted bars). This criterion indicated that *Middle-Aged* participants and the *Patient GL* were not able to catch balls with proximal part of their body (e.g., with their head) as instructed but probably only with distal part (e.g., with their arms) (mean AE equal to 0.43 vs. 0.65 m). To control that *Middle-Aged* participants and the *Patient GL* succeeded in the task by overcoming the instructions and by only attempting to intercept balls at any moment of the trials, we also computed absolute error as the minimum Euclidian distance between the agent and the ball at any moment during the overall trial course (plain bars).

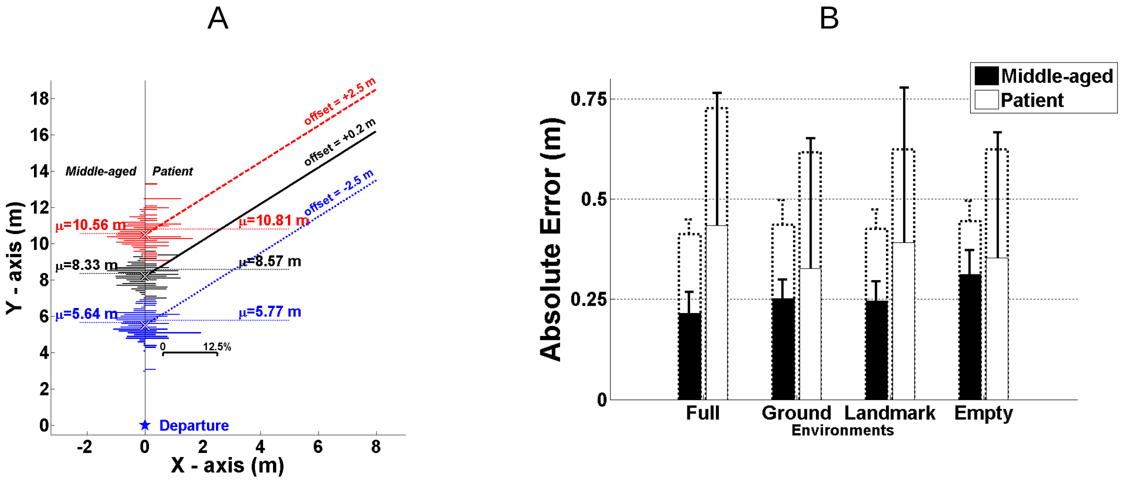

Figure 58 : (A) Frequency distribution of participant's final Y-positions (i.e., participant's positions along the Y-axis at time t=8 (s), when the ball crossed the participant's displacement axis) binned each 0.1 m and cumulated across trials performed in the four Environments conditions for the two groups of participants (Middle-Aged, Patient GL) and for the three offset conditions (-2.5, +0.2 and +2.5 m). The distributions of Middle-Aged participant's and the Patient GL's final Y-positions are depicted on the left and right sides of the displacement axis, respectively. The horizontal scale (from 0 to 12.5%) describes the frequency at which final Y-positions occurred for each bin. The average values of final Y-positions (μ) are reported and depicted with a dotted line. (B) Absolute Error plotted as a function of Environment conditions (Full, Ground, Landmark and Empty) for each Group (Middle-aged, Patient GL). Two computations of Absolute Error are displayed in B. The dotted bars depict the absolute error computed from the agent-ball distance at time t=8 (s). The plain bars represent the absolute error computed from the minimum of the agent-ball distance across the overall time-course of the trial. Vertical bars depict the standard deviation of mean values.

The Middle-Aged participants achieved an absolute error ranging from 0.21 to 0.31 m in the task (mean 0.25 ± 0.04 m). The one-way ANOVA repeated measures (4 Environments) performed on the AE mean values performed by *Middle-Aged* participants (computed with the latter definition) revealed a significant main effects of Environment ($F_{(3, 15)}$= 4.83, p>.05). Post-hoc analysis revealed that *Middle-Aged* participants were significantly more accurate in the *Full* and *Ground* environment than in the other environments (0.21 m ± 0.05, 0.25 m ± 0.05, 0.25 m ± 0.05 and 0.31 m ± 0.06 m for the *Full*, *Ground*, *Landmark* and *Empty* conditions, respectively; p<.05).

The *Patient GL* displayed an average AE ranging from 0.33 to 0.49 m (mean 0.42 ± 0.07 %m) depending on experimental conditions. A one-way ANOVA repeated measures (4 Environments) performed on the AE trial values did not reveal a significant main effect of environment ($F_{(3, 81)}$ = 0.81, p>.05). The *Patient GL* performed the task with the same AE irrespective of the Environment condition. However, her AE fell outside the 95% confidence intervals computed from the *Middle-Aged* participants in the *Full*, *Landmark* and *Empty* conditions giving rise to larger AE for this *Patient GL* than for *Middle-Aged* participants (*Full*: 0.71 vs. 0.35 m, *Landmark*: 0.60 vs. 0.43 m, *Empty*: 0.62 vs. 0.46 m). Conversely, the AE obtained by the *Patient GL* and *Middle-Aged* participants in the *Ground* condition were not significantly different (0.46 vs. 0.55 m).

Kinematics

Three-way repeated measures ANOVAs (4 Environments × 3 Offsets × 16 Time Intervals) on velocity profiles (Figure 59A) were performed separately for both groups of participants (*cf.*, Table 1).

Table 1 : Results of the three-ways ANOVA (4 Environments × 3 Offsets × 16 Time Intervals) performed on displacement velocity separately for each Groups of participants (Middle-Aged and Patient GL).

	Groups	
	Middle-Aged	***Patient GL***
Offset	$F_{(2, 10)} = 1986.46$, $p<.05$*	$F_{(2, 18)} = 320.49$, $p<.05$*
Environment	$F_{(3, 15)} = 4.25$, $p>.05$	$F_{(3, 27)} = 0.77$, $p>.05$
Time	$F_{(15, 75)} = 2.73$, $p<.05$*	$F_{(15, 135)} = 34.39$, $p<.05$*
Offset × Time	$F_{(30, 150)} = 4.62$, $p<.05$*	$F_{(30, 270)} = 1.89$, $p<.05$*
Environment × Time	$F_{(45, 225)} = 0.39$, $p>.05$	$F_{(45, 405)} = 2.56$, $p<.05$*
Offset × Environment × Time	$F_{(90, 450)} = 0.42$, $p>.05$	$F_{(90, 810)} = 1.66$, $p<.05$*

Middle-Aged participants. Analyses performed on individual mean velocity profiles revealed significant effects of Offset ($p<.05$) and Time Intervals ($p<.05$) but no significant main effect of Environment ($p>.05$). Moreover, Offset × Time Intervals ($p<.05$) interaction was also significant. *A posteriori* comparisons revealed that significantly different velocity profiles were produced in the three Offset conditions during the last 6 seconds of the trial ($p<.05$)(Figure 59). Once again the velocity changes were in accordance with the task requirements.

Patient GL. Analyses performed on trial mean velocity profiles revealed significant main effects of Offset ($p<.05$) and Time Intervals ($p<.05$). Moreover, the interactions Offset × Time Intervals ($p<.05$), Environment × Time Intervals ($p<.05$) and Offset × Environment × Time Intervals ($p<.05$) interactions were also significant. *A posteriori* comparisons revealed that the Patient GL exhibited a similar increase in velocity during the first two seconds whatever the Environment and Offset conditions ($p>.05$)(Figure 59). During the last 6 seconds, the displacement velocity profiles recorded in the *Empty* and *Landmark* conditions significantly differed between the three offset conditions (p<.05). Once again, the positive offset conditions gave rise to the higher overall velocity, the negative offset condition gave rise to the lower overall velocity, and intermediate offset conditions gave rise to intermediate velocity profiles (p<.05). Conversely, in the *Full* and the *Ground* environment conditions, the velocity profiles produced in the last 6 seconds were not significantly different (p>.05).

Taken together, these results show that the velocity profiles exhibited by *Middle-Aged* participants are highly affected by the Offset but only marginally by the Environment. Conversely the profiles produced by the *Patient GL* are affected differently by the Offset factor depending on the environment condition but greatly influenced by the Environment, with the jerkiest velocity profiles appearing in the *Full* condition. At a more descriptive level, it is also worth noting that the velocity adaptations produced by *Middle-Aged* participants were not smooth. In particular, the displacement velocity adjustments produced by the *Patient GL* are highly non linear in particular in the *Full* condition, i.e., when both optic flow and retinal signals are available.

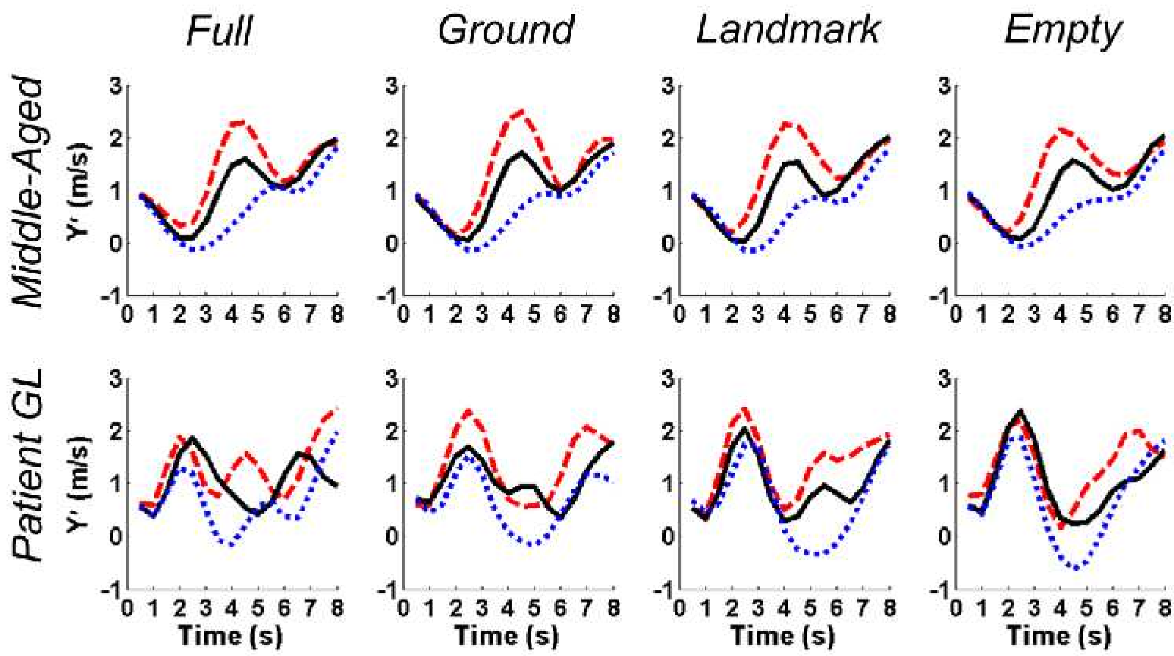

Figure 59 : Velocity profiles exhibited by the two groups of participants (Middle-Aged and Patient GL) in the four environment conditions (*Full*, *Ground*, *Landmark* and *Empty*) and in the three offset conditions (Dotted, plain and dashed lines for the -2.5, +0.2 and +2.5 m offset conditions, respectively).

We further analyzed the displacement kinematics by counting the number of zero crossings exhibited in the acceleration profiles ($ZC_{\ddot{Y}}$). The number of $ZC_{\ddot{Y}}$ is indicative of whether the displacement adaptations are gradual (very few $ZC_{\ddot{Y}}$) or conversely nonlinear (numerous $ZC_{\ddot{Y}}$)(Figure 60).

One-way ANOVA (4 Environments) with repeated measures on the Environment factor performed on the individual mean number of $ZC_{\ddot{Y}}$ performed by *Middle-Aged* participants dot not revealed a significant main effect of the Environment factor ($F_{(3,\ 15)} = 0.03$, p>.05). One-way ANOVA (4 Environments) with repeated measures on the Environment factor performed on the trial mean number of $ZC_{\ddot{Y}}$ performed by the *Patient GL* dot revealed a significant main effect of the Environment factor ($F_{(3,\ 81)} = 2.18$, p>.05). Finally, the number of ZC produced by the *Patient GL* fell outside the 95% confidence interval computed from *Middle-Aged* participants in all the Environment conditions, giving rise to a larger trial mean value of ZC for the *Patient GL* than for *Middle-Aged* participants (3.70 ± 0.24 *vs*.2.47 ± 0.07).

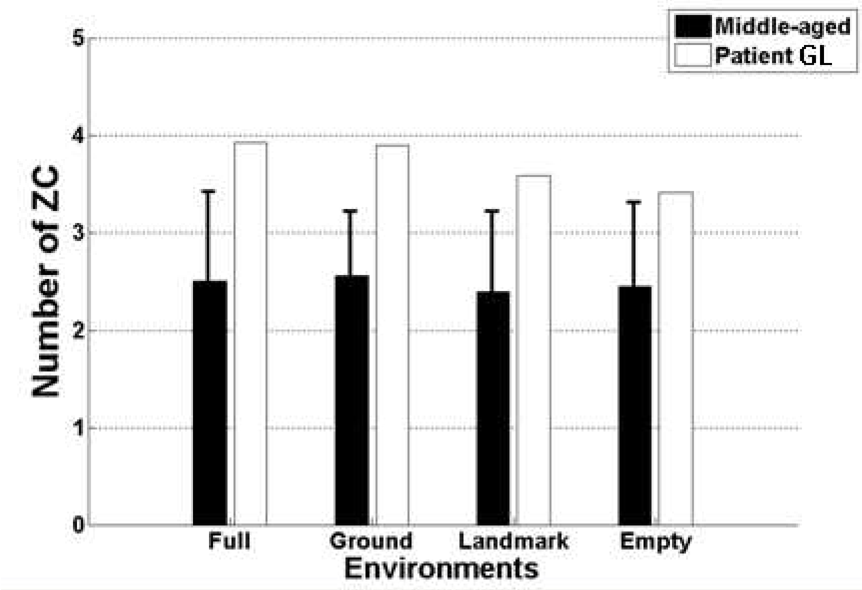

Figure 60: Number of zero crossings acceleration occurrence ($ZC_{\ddot{Y}}$) plotted as a function of Environment conditions (Full, Ground, Landmark and Empty) for each Group (Middle-aged, Patient GL). Vertical bars depict the standard deviation of mean values.

Perceptual-motor strategy

First, analyses were based on systematic comparisons between the mean velocity profiles produced by each group of participants and the best fitting numerical simulations provided by the CBA model. Numerical simulations of the CBA model (dotted lines, Figure 61) failed to approximate the regulation behavior exhibited by both *Middle-Aged* ($R^2 < 0.46$) and the *Patient GL* ($R^2 < 0.52$) as found y Francois et al. (in press). In particular, it appears that the CBA model cannot account for their non-gradual velocity profiles (Figure 61).

Second, analyses were based on systematic comparisons between the mean velocity profiles produced by each group of participants and the best fitting numerical simulations provided by the 'Bounded-CBA' model (Equation 2) formulated by Francois et al. (in press). The 'Bounded-CBA' rests on a neuro-physiologically grounded control architecture. According to this model, a change in bearing angle gives rise to a behavioral adaptation provided the angular changes are greater than a threshold that is known to increase with ageing (Andersen & Enriquez, 2006; Tran, Silverman, Zimmerman, & Feldon, 1998; Warren, Blackwell, & Morris, 1989). Conversely, when angular changes do not exceed the threshold, the system maintains the previous state. More precisely in the 'Bounded-CBA' model, the ratio between the current value of the rate of change in bearing angle $\dot{\theta}$ and an assumed perceptual threshold $\dot{\theta}_t$ acts as a switch function. When the absolute value of the ratio $\dot{\theta}/\dot{\theta}_t$ exceeds 1, then the acceleration of the participant ($\ddot{Y}$) is driven by the rate of change in bearing angle and the damping of the system. If the absolute value of the ratio $\dot{\theta}/\dot{\theta}_t$ is less than 1, then the simulated acceleration ($\ddot{Y}$) continues to be gradually driven by the acceleration prescribed at $t-1$.

$$\ddot{Y} = \begin{cases} k_1 \times \dot{\theta} \times \dfrac{1}{1+200 \times e^{(-10 \times t)}} + k_2 \times \dot{Y}, if \left|\dot{\theta}/\dot{\theta}_t\right| > 1 \\ \ddot{Y}_{t-1}, if \left|\dot{\theta}/\dot{\theta}_t\right| < 1 \end{cases} \qquad \text{Equation 2}$$

According to this architecture, for a given set of initial conditions, higher perceptual thresholds should give rise to jerky velocity changes, while low thresholds should give rise to smooth regulations. A best-fitting procedure identical to the one used for the CBA model was applied to the 'Bounded-CBA' model using a similar range of k_1 and k_2 parameters.

Moreover we also included a search on the perceptual threshold parameter ($\dot{\theta}_t$) ranging from 0°/s to 4°/s with 0.05°/s increments.

Figure 61 shows the best-fitting numerical simulations provided by the “Bounded-CBA” model (Equation 2) for each group of participants and for each Environment condition in the + 0.2m offset condition. The “Bounded-CBA” model provides a good account of the velocity profiles for the *Middle-Aged* participants and for the *Patient GL* and in the different environment conditions (R^2 mean values equal to 0.72 and 0.72). Interestingly, the best perceptual thresholds values accounting for the regulation behavior of *Middle-Aged* participants did not vary very much across the environment conditions ($2.3 < \dot{\theta}_t < 2.5$ °/s). Conversely, the environment conditions influenced the perceptual threshold for the *Patient GL*. While the perceptual thresholds were comparable for the *Patient GL* and the *Middle-Aged* participants in the *Full* condition (2.3 vs. 2.5°/s), the impoverishment of the environment was accompanied by an increase in the perceptual threshold (e.g., 2.3, 2.4, and 2.7 °/s in the *Full*, *Ground*, *Landmark* and *Empty* conditions, respectively for the +0.2 offset condition).

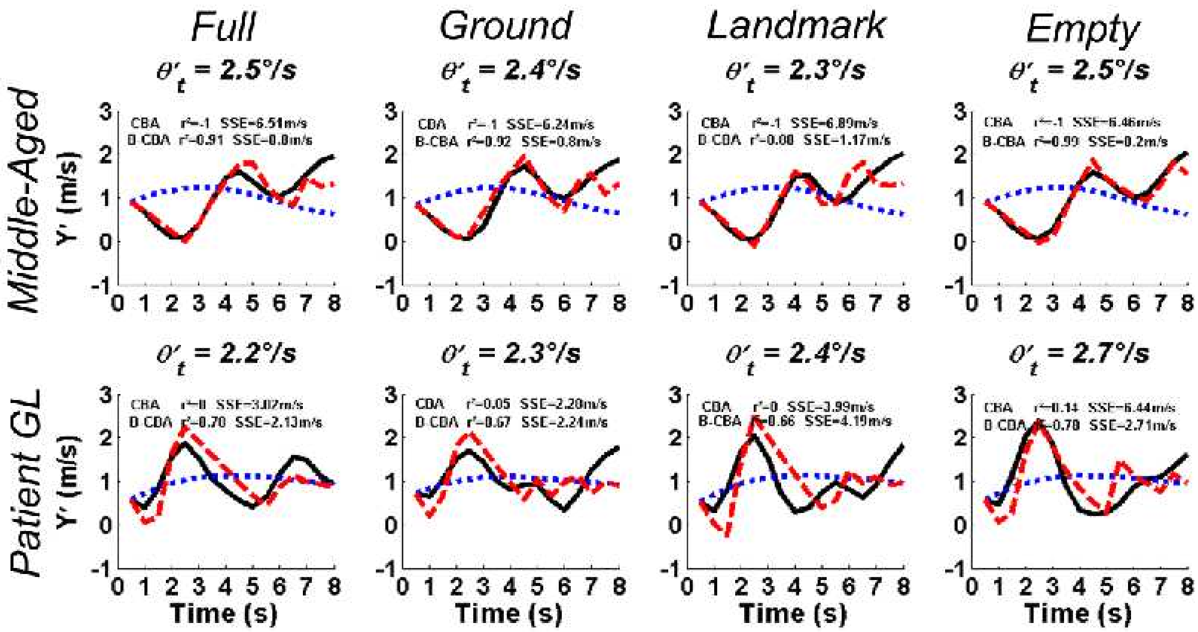

Figure 61: Best fitting numerical simulations of the average observed velocity provided by the two models (dotted and dashed lines for the CBA and ‘Bounded-CBA’ numerical simulations, respectively) for the two Groups of participants (Middle-Aged, Patient GL) in the different Environment conditions (*Full*, *Ground*, *Landmark* and *Empty*) for the +0.2 m offset condition. The R^2 and Sum of Square Error (SSE) corresponding to each model are included, together with the perceptual threshold providing the best fit ($\dot{\theta}_t$).

DISCUSSION

The aim of the Experiment was to determine to what extent deafferentation affected the human ability to intercept moving balls depending on visual sources of information contained in the environment. We asked two groups of participants (*Middle-Aged*, *Patient GL*) to intercept balls that travelled toward them obliquely in a virtual environment by manipulating a joystick allowing them to control their velocity. More precisely, we set-out an experiment in which different visual information specifying the direction of displacement were drained form the visual environment, leading finally participants to rely on proprioceptive information. In the *Full* Environment, the visual scene contained two visual information related to the direction of displacement: the FoE and a visual egocentric frame of reference. In the *Ground* Environment, only the FoE was available. In the *Landmark* Environment, only a visual egocentric frame of reference was available. In the *Empty* environment, the visual scene do not allowed to determine one's the direction of displacement on the basis of visual signals.

Analyses of performance (AE) revealed that the *Patient GL* achieved worse score than her healthy counterparts (*Middle-Aged* Participants). Moreover, whereas the performances of Middle-aged participants were damaged as the environment was drained from its visual content (*Full*, *Ground*, *Landmark* and *Empty*), the *Patient GL* was able to keep constant its performances in all Environments. *Middle-Aged* Participants produced a better AE than the *Patient GL* in three of the four environment conditions (i.e., *Full*, *Landmark* and *Empty* conditions). Kinematics analyses showed that the *Patient GL* exhibited jerkier velocity profiles than *Middle-Aged* participants. Moreover, whereas the velocity profiles performed by *Middle-Aged* participants do not differed between Environment conditions, the *Patient GL* exhibited jerkier velocity profiles in particular when the three types of perceptual signals (i.e., visual allocentric, visual egocentric, proprioceptive egocentric) were available (*Full* condition). The CBA model failed to explain the behavior observed by the *Middle-Aged* participant and the *Patient GL*. Interestingly however, adding adjusted perceptual thresholds in the numerical simulations allowed the 'Bounded-CBA' model to provide a good account of the behavior produced by the three groups of participants in all environment conditions.

The influence of deafferentation

The core issue of the present work is the evaluation of the interceptive performance when the egocentric reference system is greater impaired by the absence of proprioceptive signals. The three levels of analysis (Performance, Kinematics and Perceptual-Motor strategy) provide complementary pieces of answer. First of all, in comparison with *Middle-Aged* participants the *Patient GL* produced a lower performance in three out of the four environment conditions (*Full*, *Landmark* and *Empty*). While this result was expected in the *Empty* condition, we expected the *Patient GL* to be as accurate as *Middle-Aged* participants in the presence of visual information, i.e., in the other three conditions. Moreover, contrary to our expectations, the *Patient GL* reached the same level of performance when visual information was lacking (i.e., *Empty* condition) and when the environment was visually enriched.

The kinematic analyses performed on displacement kinematics provide some insights into these unexpected results. These analyses confirm previous studies; the displacement velocity profiles produced by both *Middle-Aged* and Deafferented patients are highly jerky (Riviere & Thakor, 1996). These jerky velocity profiles are even more pronounced for the Patient GL, in particular in the *Full* condition, i.e., when visual information is available through both optic flow and retinal signals.

Finally, the analyses on the perceptual-motor strategies enable us to clarifying the picture one step further. The initial version of the Constant Bearing Angle model failed to account for the regulation behavior produced by the *Patient GL*. Conversely, this study confirms the need for neuro-physiologically grounded architecture of law of control. As found by Francois et al. (in press), the ‘Bounded-CBA’ model allowed accounting for jerky velocity profiles performed by *Middle-Aged* participants, revealing thus that perceptual threshold for perceiving $\dot{\theta}$ drove the control of displacement. Moreover, our study also revealed that the ‘Bounded-CBA’ model allowed accounting for velocity profiles performed by the *Patient GL*. Consequently, the sudden and steep slope in the displacement adaptations could express the patient’s difficulties to detect small angular changes. This could have led her to ‘bounce’ from the upper part of the threshold to the lower part of the threshold. Interestingly the perceptual thresholds found for the *Patient GL* differed across the environment conditions (2.3, 2.6, 2.8 and 2.8 °/s for the *Full*, *Ground*, *Landmark* and *Empty* conditions respectively). In the *Full* condition, the patient’s threshold is not only minimal, but is also of the same magnitude as the threshold found for *Middle-Aged* participants. This result suggests that, when available, optic flow and retinal signals compensate for the lack of extra-retinal signals in detecting the rate of change in bearing angle. The reason why this condition did not give rise to an increase in performance is probably related to the constraints imposed to the participant and in particular to the impossibility to see both the hand and the joystick.

Surprisingly the *Patient GL*'s performance did not decrease when both optic flow and retinal (i.e. the body-centered cross on the screen) information were removed. This result was unexpected given that the *Patient GL* suffers from a lack of proprioception from the neck muscles and that this information greatly contributes to determine object position and motion relative to the body (Biguer, Donaldson, Hein, & Jeannerod, 1988; Taylor & McCloskey, 1991). Although head position and muscular activity were not recorded in the present experiment, we could clearly notice that the *Patient GL* kept her head directed towards the ball, possibly by stiffening of her trunk and neck muscles. Freezing body segments is a common strategy of patients and *Middle-Aged* individuals with sensory impairments (Benjuya, Melzer, & Kaplanski, 2004; Bloem, Allum, Carpenter, Verschuuren, & Honegger, 2002; Lajoie et al., 1992). Having both the head and gaze directed towards the ball, the *Patient GL* may have compensated perceptible changes in gaze direction (i.e., in bearing angle) by accelerating or decelerating accordingly. Within this framework, sensorimotor signals originating from the extra-ocular muscles (Gauthier, Nommay, & Vercher, 1990) would have an important role to detect the rate of change in the bearing angle. Relying essentially on these signals, the *Patient GL* would be able to perform the task with a reasonable accuracy in comparison with the other environment conditions.

CONCLUSION

This study confirms the need for neuro-physiologically grounded architecture of law of control but do not jeopardize the status of the Constant Bearing Angle strategy as a perceptual-motor principle being able to account for the regulation behavior of participants. More precisely, perceptual constraints added in numerical simulations of the 'Bounded-CBA' model perfectly fit with the 'perception actuation' level of analysis suggested by Bootsma (Bootsma, 1998). This study also reveals the perceptual problem encountered by Deafferented patients, whose perceptual systems allow them to be able to exploit redundant visual perceptual variables and switch from visual allocentric variables to egocentric ones. However, this study revealed the importance of proprioceptive signal for the control of interception in impoverished visual environments, providing thus converging results with previous study (Bastin et al., 2006a).